# A NUMERICAL SIMULATION OF SINGLE BUBBLE GROWTH PROCESSES IN SATURATED AND SUBCOOLED NUCLEATE BOILING WATER

Ning CHENG[1], Yun GUO[1], Changhong PENG [1], Yong ZHANG[2, 3]
1. School of Nuclear Science and Technology, University of Science and Technology of China, Hefei, Anhui, 230026, China
2. Science and Technology on Reactor System Design Technology Laboratory, Nuclear Power Institute of China, Chengdu 610213, China;
3. Nuclear Power Institute of China, Chengdu, 610213, China;
Corresponding author: Changhong PENG, e-mail: pengch@ustc.edu.cn

REFERENCE NO

FUSN-01

*Keywords:*
Numerical simulation, Bubble growth, Saturated boiling, Subcooled boiling, VOF method

ABSTRACT

Numerically investigated the processes of single bubble growth in saturated and subcooled nucleate boiling water using volume of fluid (VOF) method in commercial software ANSYS FLUENT under two-dimensional condition. A phase change model was adopted by adding extra mass source term and energy source term to the Navier-Stokes equation in the cells who were adjacent to the vapour-liquid interface. The simulation results were compared with data in previous literature to verify the validity. The bubble contour variations, heat flow distributions, temperature fields, velocity fields and mass source distributions in saturated and subcooled nucleate boiling water were obtained and compared.

## 1. INTRODUCTION

Water-cooling blanket is an important component in future fusion reactor and is closely related to reactor system safety for it can cool the reactor down. Nucleate boiling may occur in water-cooling blanket during the cooling process, although it can improve heat transfer efficiency, sometimes it may lead to critical heat flux (CHF) and burn out the wall. The bubble growth process is a basic problem in nucleate boiling. So it's necessary to research the bubble growth process in nucleate boiling water for the safety of reactor.

Since the last century, many researches have been done to research the bubble growth process while it remain unclear, and most of the studies only concentrate on saturated condition or subcooled condition without contrast. In this paper two cases of single bubble growth processes in saturated and subcooled boiling water have been numerically investigated corresponding to the experiments in reference [1] and [2].

Fig.1 (a) and Fig.1 (b) present a bubble generating on a horizontal surface in saturated and subcooled boiling water respectively. Where $Q_{bf}$ is the energy released by bubble cap in subcooled fluid and is equal to 0 in saturated case; $Q_{sl}$ stands for the energy absorbed by bubble in superheated liquid layer; $Q_{ml}$ accounts for the energy absorbed by micro-layer due to evaporation; $Q_c$ indicates the energy absorbed by bubble cap and $Q_t$ indicates the total energy, the relationships between them are:

$$Q_c = Q_{sl} - Q_{bf} \quad (1)$$

$$Q_t = Q_{ml} + Q_{sl} - Q_{bf} \quad (2)$$

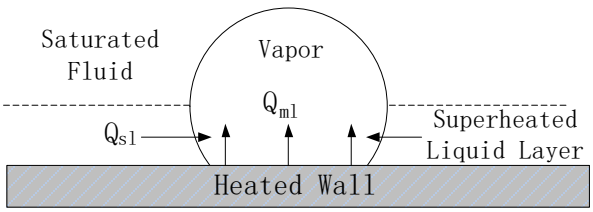


(a)

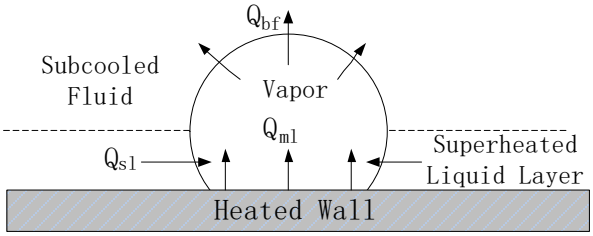


(b)

Fig.1 Single bubble growth processes in saturated boiling water (a) and subcooled boiling water (b)

## 2. THEORETICAL METHOD

The equations need to be solved in calculations are the conservation equations for mass, energy, momentum and volume fraction:

$$\rho \nabla \cdot \boldsymbol{u} = \dot{\rho} \tag{3}$$

$$\frac{\partial pcT}{\partial T} + \nabla \cdot (\boldsymbol{u} \cdot \rho cT) = \nabla \cdot (\lambda \cdot \nabla T) + \dot{h} \tag{4}$$

$$\frac{\partial \rho \boldsymbol{u}}{\partial T} + \nabla(\boldsymbol{u} \cdot \rho \boldsymbol{u}) = -\nabla p + \nabla \cdot (\mu \cdot \nabla \boldsymbol{u}) + S_s + S_g \tag{5}$$

$$\frac{\partial \alpha_v}{\partial t} + \nabla \cdot (\boldsymbol{u} \cdot \alpha_v) = \frac{\dot{\rho}}{\rho} \alpha_v \tag{6}$$

Where $\rho$ is the density, $\nabla$ is the laplacian operator, $\boldsymbol{u}$ is the velocity vector, $\dot{\rho}$ represents the mass transition caused by the phase change, $c$ is the specific heat capacity, $T$ and $t$ are the temperature and time, $\dot{h}$ indicats the change of energy during the phase transition, $P$ is the pressure, $\alpha_v$ is the volume fraction of vapour phase, $S_s$ and $S_g$ are the surface tension force [3] and gravity force respectively. For the cells at the liquid-vapour interface, the physical parameters are calculated by the weighted average of the volume fraction.

The phase change model proposed by Lee [4] was adopted in the simulation. In this model, the occurrence of phase change depends on local temperature $T$ and saturation temperature $T_{sat}$. When the local temperature at liquid-vapour interface is higher than saturation temperature ($T > T_{sat}$), evaporation occurs; when the local temperature at liquid-vapour interface is lower than saturation temperature ($T < T_{sat}$), condensation occurs. The conversion of phase is achieved by adding extra mass and energy source terms to the Navier-Stokes equation. The mass source terms are written as Eq. (7) and Eq. (8). The energy source term can be got by multiplying the mass source with the phase change latent heat as shown in Eq. (9):

$$M = c_l \alpha_l \rho_l \frac{T - T_{sat}}{T_{sat}} \quad (T > T_{sat}) \tag{7}$$

$$M = c_l \alpha_l \rho_l \frac{T - T_{sat}}{T_{sat}} \quad (T < T_{sat}) \tag{8}$$

$$\dot{h} = h_l M \tag{9}$$

Where $M$ can be written as $M_l$ or $M_v$, representing liquid phase mass source and vapour phase mass source respectively. $\alpha_l$ indicates the volume fraction of the liquid phase, $c_l$ and $c_v$ are time relaxation factors and $h_l$ is the latent heat of phase change.

In two-dimensional calculation, if $M_v$ is added to the cells who contain liquid-vapour interface directly, the calculation will result in distortion of the interface. So the position of $M_v$ should be adjusted to the cells who are adjacent to the liquid-vapour interface in the vapour phase in order to ensure the clarity and sharpness of the bubble boundary during the calculation.

## 3. NUMERICAL SIMULATION

The computational domain consists of a fluid region and a solid region as shown in Fig.2. In the simulation, the fluid region was subdivided into zone 1 and zone 2. The connection line between the two zones was defined as the interior boundary. The top of the computational domain was set as pressure outlet and the back flow temperature was equal to the mainstream temperature. The left and right sides of the calculation region were set as walls. The nucleation site was located at the centre of the upper surface on the substrate. The scale of cells was set as 40 μm × 40 μm and the time step was $10^{-5}$ s to ensure that the Courant number was small enough.

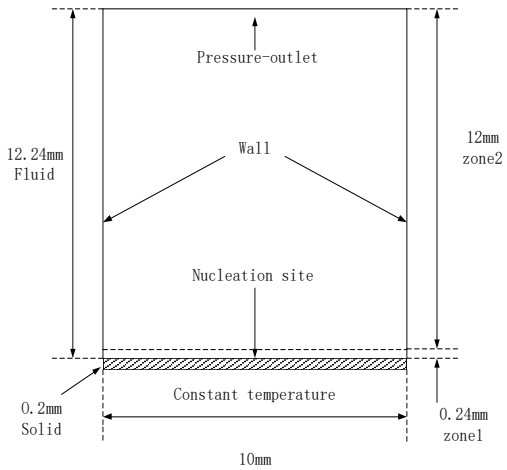


Fig.2 The schematic diagram of computational domain

The settings of the parameters in numerical simulation is the same as those in literature [1] and [2]. In the saturated case, the temperatures of main fluid and heating wall were set as 373K and 383.8K, and the contact angle was 60 ° according to reference [1]. They would be constant during the calculation for the bubble growth process only took few milliseconds. In order to obtain an initial state, the velocity field in computational domain was set as zero and the pressure was set as standard atmospheric pressure. The bubble growth rate no longer increased when the bubble height reached 1.5 mm in the experiment, so the height of superheat layer was considered to be 1.5 mm. The fluid was heated by the bottom. When the temperature of fluid at the height of 1.5 mm just reached the saturation temperature, a small bubble whose radius was 0.2 mm was placed at the nucleation point to simulate the initial state. Then the bubble would grow by evaporation. Similarly, in the subcooled case, the fluid temperature was set as 363K, the heating wall temperature was set as 388.8K and the contact angle was 60 °. The velocity field in the computational domain was set as zero and the pressure was set as standard atmospheric pressure. When the height of superheated liquid layer reached 1.7mm, a small bubble with a radius of 0.2 mm was placed at the nucleation point. Then the bubble would grow by evaporation.

There is a micro-layer whose thickness is only few micrometres between the bubble and the wall according to reference [5]. The thickness of the micro-layer is tiny while the initial evaporation is extremely strong, so it is difficult to simulate it directly. To simulate the evaporation of micro-layer, a vapour mass source whose temperature is equal to the wall temperature is added to the vapour phase in zone 1 referring experimental results in the calculation.

## 3. CALCULATION RESULTS

### 3.1. Bubble contours

Fig. 3 (a) and (b) present the bubble contours (The isoline of $\alpha_v$ = 0.5) got by simulation and the experiment in reference [1] under saturated condition. Fig.4 (a) and (b) show the bubble contours obtained by simulation and the experiment in reference [2] under subcooled condition. The simulation results are shown in a square of 6 mm × 6 mm in each figure. It can be observed that the change trends of bubble profiles obtained by numerical simulation are in good agreement with the experiment results. In both groups of pictures, the bubble contour changes from a flat ellipse to a truncated circle and finally to a pear shape. While some differences still exist, the bubble volume is continuously increasing under saturated condition but it first increases then decreases under subcooled condition.

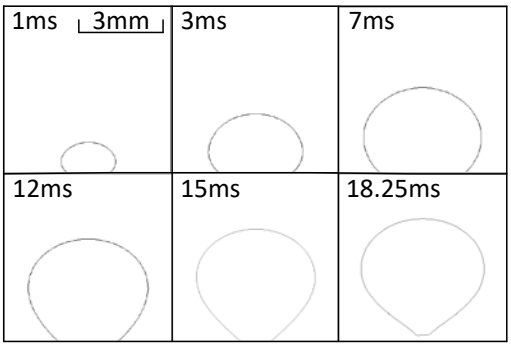


(a)

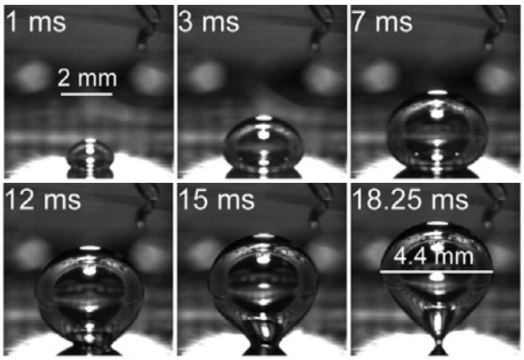


(b)

Fig.3 Bubble contours got by simulation (a) and experiment (b) in saturated case

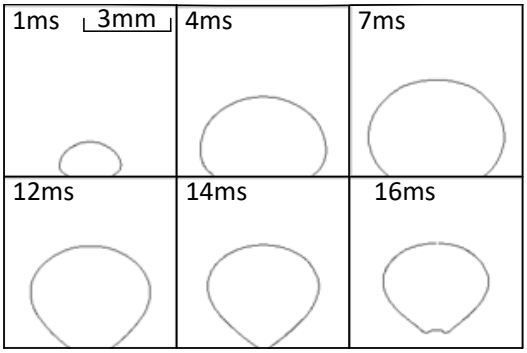


(a)

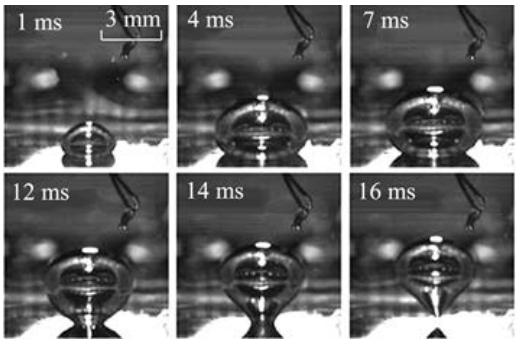


(b)

Fig.4 Bubble contours got by simulation (a) and experiment (b) in subcooled case

Fig.5 (a) and (b) show the maximum bubble diameter and height change trends got by simulation and experiment in two cases. It can be seen that in saturated case the maximum bubble diameter and height continuously increase. In subcooled case, the bubble height increases continuously, while the maximum bubble diameter first increases then decreases.

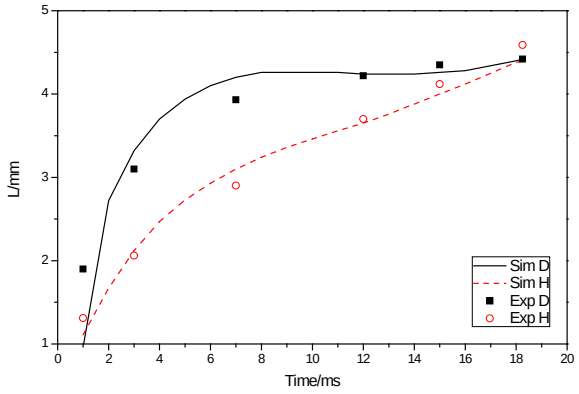


(a)

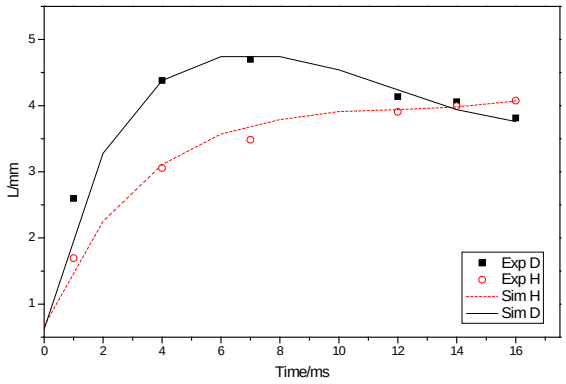


(b)

Fig.5 Bubble maximum diameter and height variations in saturated case (a) and subcooled case (b)

### 3.2. Heat flows

Fig.6 (a) and (b) show the variations of $q_{ml}$, $q_c$ and $q_t$ in two cases. The $q$ is determined as heat flows, $q_{ml}$, $q_c$ and $q_t$ are calculated by temporal differentiation of $Q_{ml}$, $Q_c$, and $Q_t$ respectively. It can be found that $q_{ml}$, $q_c$ and $q_t$ have similar tendency in two pictures: At first the $q_{ml}$ increases due to the extension of the bubble base in both cases, then it decreases for the shrinkage of contact area and the expansion of dryout region until bubble departure. As for $q_c$, it has positive value for most of the bubble is immersed in superheated liquid layer at initial stage, then more bubble cap is exposed to saturated /subcooled water with the growth of the bubble and $q_c$ became smaller/negative. And $q_t$ is the sum of $q_{ml}$ and $q_c$.

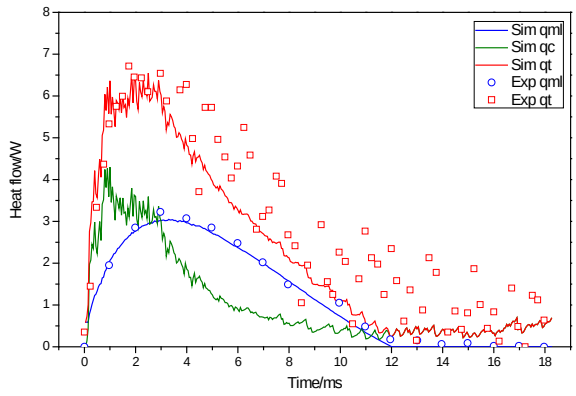


(a)

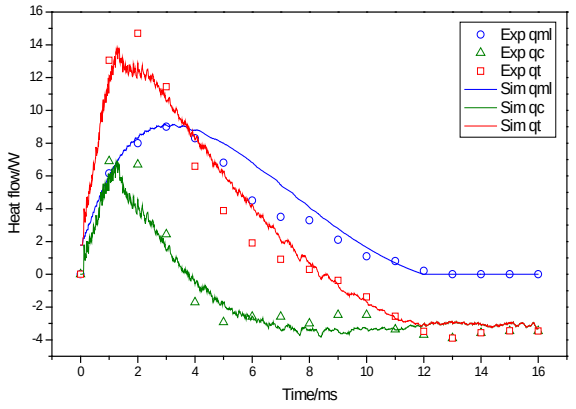


(b)

Fig.6 Heat flows obtained by simulation and experiment in saturated case (a) and subcooled case (b)

### 3.3. Temperature fields and velocity fields

The temperature fileds which cannot be measured directly by experiment in saturated and subcooled cases are presented in Fig.7 (a) and (b). In each case, the temperature of extra vapour source added at zone 1 is pre-assumed as equal to the wall temperature. Therefore, the temperature inside the bubble is higher than saturation temperature. And the liquid-vapour interface always stays around the saturation temperature for mass change is occurring there. The energy absorbed/released by phase change process can keep the temperature stable.

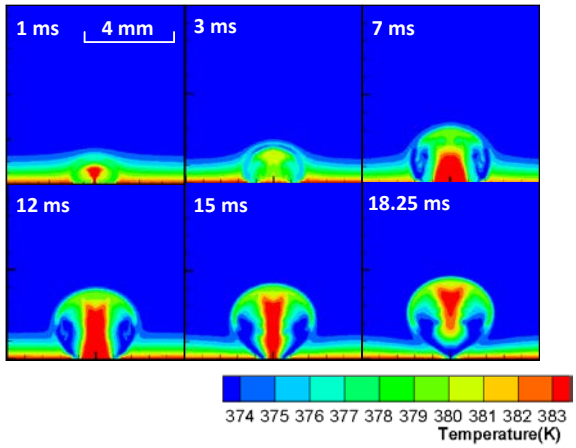


(a)

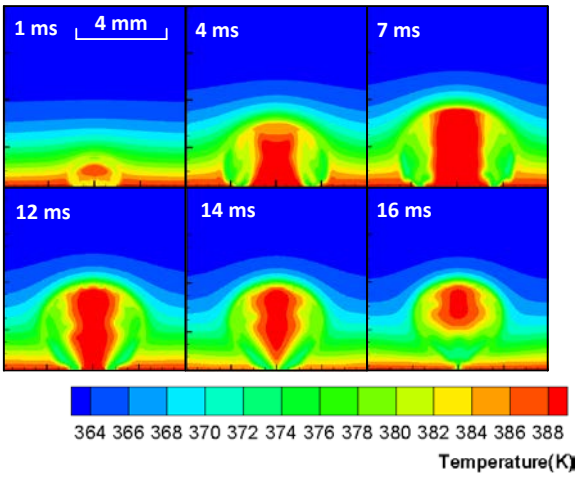


(b)

Fig.7. Temperature fields in saturated case (a) and subcooled case (b)

In Fig.8 (a) and (b), the velocity fields have similar change trends in both cases. At initial stage, the direction of velocity point out of interface from the inside of the bubble for the bubble is growing dramatically in this period. Then two week whirlpools generate in the bubble attached to interface on the left and right sides. Because the steam flow generated by bubble base rises from the bubble centre, then it changes direction and streams along the interface, but it can't extend to the bottom for new vapour is generating there, thus the vapour circulate in the bubble.

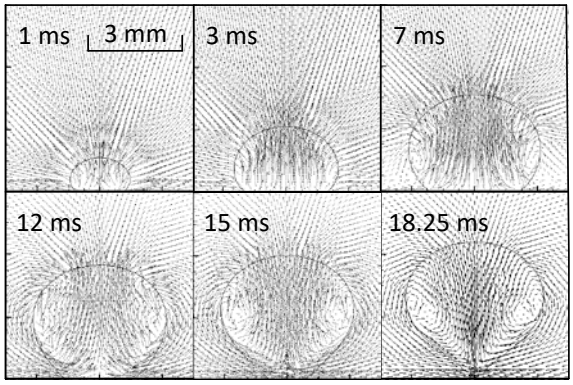


(a)

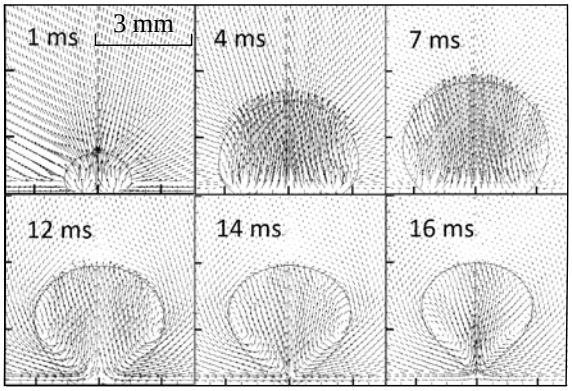


(b)

Fig.8. Velocity fields in saturated case (a) and subcooled case (b)

### 3.4. Vapour mass sources

Fig.9 (a) and (b) present the distributions of vapour mass source in saturated case and subcooled case respectively. As can be seen in Fig.9 (a), at the early stage of bubble growth, the evaporation is dramatically for the bubble is totally submerged in superheated liquid layer. Then it will gradually weakened and there is no obvious evaporation on the bubble cap submerged in the saturated mainstream. For the subcooled case in Fig.9 (b), at first vigorous evaporation occurs at the bubble boundary just like Fig.9 (a). Then there are obvious evaporation occurring at the bottom of the bubble cap and obvious condensation occurring at the top of bubble cap. With time goes by, the degrees of evaporation and condensation both decrease for the energy absorbed/released by phase change makes the local temperature closer to saturation temperature at the interface. Finally they will be much weaker when bubble is departing.

To avoid the deformation of liquid-vapour interface during the calculation, the vapour mass sources have been added to the cells who are adjacent to the interface in the vapour phase but not the cells who exactly contain two phase. This adaptation can keep the surface clear and sharp in two-dimensional VOF calculation.

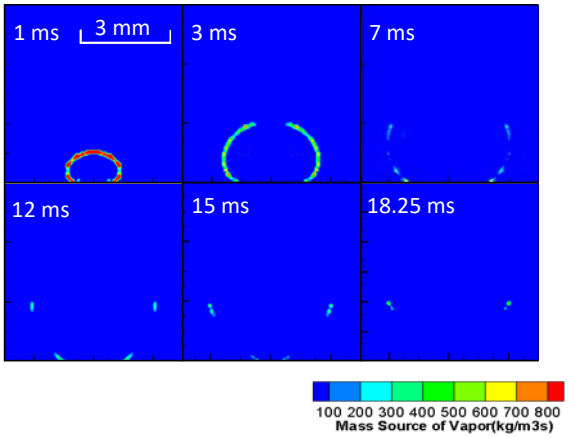


(a)

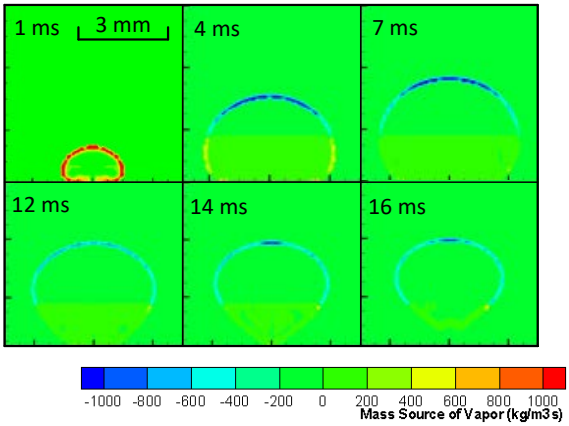


(b)

Fig.9. Vapour mass source distributions in saturated case (a) and subcooled case (b)

## 4. CONCLUSIONS

In this work, the processes of single bubble growth in saturated and subcooled nucleate boiling water were numerically investigated and the simulation results fitted well with the experimental data. Two conclusions can be drawn from this work:

1. For the bubbles generated in saturated and subcooled nucleate boiling water, the temperature fields and velocity fileds in two cases have similar change trends. The bubble inner temperature is higher than saturation temperature and the liquid-vapour interface always stays around the saturation temperature. The vapour rises in the bubble

centre and flows down along the bubble surface resulting two week whirlpools on the left and right sides in the middle part of the bubble. While some differences still exist between two cases in bubble contours, heat flows and mass source distributions.

2. The adjustment of vapour mass source from the cells who exactly contain two phase at the interface to the cells who are adjacent to the interface in the vapour phase can avoid the deformation of bubble shape and keep the liquid-vapour interface clear and sharp in the simulation.

**Acknowledgements**

This study is supported by National Natural Science Foundation of China (Grant No. 11305169); the National Magnetic Confinement Fusion Science Program of China (Grant No. 2013GB108004) and the National Special Project for Magnetic Confined Nuclear Fusion Energy (No.2017YFE 0300604).

**Nomenclature**

| | |
|---|---|
| $Q_{bf}$ | The energy released by bubble cap in mainstream (J) |
| $Q_{sl}$ | The energy absorbed by bubble cap in superheated liquid layer (J) |
| $Q_{ml}$ | The energy absorbed by micro-layer(J) |
| $Q_c$ | The energy absorbed by bubble cap (J) |
| $Q_t$ | The total energy (J) |
| $\boldsymbol{u}$ | Velocity vector (m/s) |
| $c$ | Specific heat capacity (J/kg K) |
| $T$ | Temperature (K) |
| $t$ | Time (s) |
| $\dot{h}$ | The change of energy during the phase transition (J/m$^3$s) |
| $P$ | Pressure (Pa) |
| $S_s$ | Surface tension force (N) |
| $S_g$ | Gravity force (N) |
| $T_{sat}$ | Saturation temperature (K) |
| $M$ | Mass source (kg/m$^3$s) |
| $M_l$ | Mass source of liquid (kg/m$^3$s) |
| $M_v$ | Mass source of vapour (kg/m$^3$s) |
| $c_l$ | Relaxation time factor (1/s) |
| $c_v$ | Relaxation time factor (/s) |
| $h_l$ | The latent heat (J/kg) |
| $q_{ml}$ | The heat flow absorbed by micro-layer (W) |
| $q_c$ | The heat flow absorbed by bubble cap (W) |
| $q_t$ | The total heat flow (W) |

**Greek Letters**

| | |
|---|---|
| $\alpha_v$ | Volume fraction of vapour phase |
| $\alpha_l$ | Volume fraction of liquid phase |
| $\rho$ | Density (kg/m$^3$) |
| $\dot{\rho}$ | The mass transition (kg/m$^3$s) |

**References**

[1] T. Yabuki, O. Nakabeppu. Heat transfer mechanisms in isolated bubble boiling of water observed with MEMS sensor. *International Journal of Heat and Mass Transfer*, 2014, 76,286–297.

[2] T. Yabuki, O. Nakabeppu. Microscale wall heat transfer and bubble growth in single bubble subcooled boiling of water. *International Journal of Heat and Mass Transfer*, 2016, 851-860.

[3] J.U. Brackbill, D.B. Kothe, C. Zemach. A continuum method for modeling surface tension,. *Comput. Phys*. 1992, 335–354.

[4] W.H.A Lee. Pressure iteration scheme for two-phase flow modeling. In: Veziroglu, T.N. (Ed.), Multiphase transport fundamentals, Reactor Safety, Applications. Hemisphere Publishing, Washington, D. C, 1980.

[5] S. Jung, H. Kim. An experimental method to simultaneously measure the dynamics and heat transfer associated with a single bubble during nucleate boiling on a horizontal surface. *International Journal of Heat and Mass Transfer*, 2014, 73, 365–375.